J. Physiol. (1985), **364**, *pp.* 217–239
With 12 text-figures
Printed in Great Britain

A CALCIUM-ACTIVATED CHLORIDE CURRENT GENERATES THE AFTER-DEPOLARIZATION OF RAT SENSORY NEURONES IN CULTURE

BY MARK L. MAYER*

From the Laboratory of Developmental Neurobiology, NICHD, Building 36, Room 2A21, National Institutes of Health, Bethesda, MD 20205, U.S.A. and Department of Pharmacology, St. George's Hospital Medical School, Cranmer Terrace, London SW17 0RE

(*Received 20 November 1984*)

SUMMARY

1. Neurones from the dorsal root ganglia of 1-day-old rat pups were grown in dissociated culture and voltage clamped using patch electrodes for whole-cell recording. The pipettes were filled with either 140 mM-KCl or CsCl.

2. Depolarizing voltage jumps activated net inward calcium currents in all neurones, which in a subpopulation of 46 % were followed by slowly decaying inward tail currents accompanied by large increases in membrane conductance. During voltage jumps to membrane potentials more positive than 0 mV the inward calcium current was contaminated by a slow outward relaxation only in those neurones with slow inward tail currents. The availability curve for the slow inward tail current was U shaped, with a peak at approximately +5 mV in medium containing 2·5 mM-Ca^{2+}; further depolarization reduced the amplitude of the tail current.

3. During perfusion with calcium-free solution, or in the presence of the calcium-channel blockers cadmium or cobalt, or on substitution of barium for calcium, both the slow inward tail currents and outward relaxations were reversibly blocked.

4. The reversal potential of the slow inward tail current, measured using a twin-pulse protocol, was approximately −10 mV. Replacement of sodium by tetraethylammonium (TEA) did not reduce the slow inward tail current, nor change its reversal potential. Reduction of the extracellular chloride activity produced a large increase in the amplitude of the slow inward tail current suggesting an increase in permeability to anions. This conductance, which behaves as though activated by prior or concurrent calcium entry triggered by membrane potential depolarization, is referred to as $I_{Cl(Ca)}$.

5. The activation and deactivation kinetics of $I_{Cl(Ca)}$ are complex: envelope experiments measuring peak tail current amplitude revealed activation to be described by a single exponential function, of time constant approximately 100 ms at −10 to +8 mV. The integral of the tail currents increased with the duration of depolarizing pre-pulses suggesting accumulation of intracellular calcium. The decay

* Beit Memorial Fellow.

of tail currents activated by short depolarizing voltage jumps was described by a single exponential function of time constant approximately 200 ms at −60 mV; more complex decay kinetics were recorded following activation by voltage jumps of duration greater than 60 ms. Tail current decay was voltage sensitive, becoming faster with hyperpolarization and increasing e-fold per 120 mV change in membrane potential.

INTRODUCTION

Chick sensory ganglion cells in culture fire action potentials followed by long-duration spike after-depolarizations (Crain, 1971; Dichter & Fischbach, 1977). The mechanism underlying this response has not been resolved. Crain (1971) suggested that sensory neurone axon collaterals form excitatory synapses with adjacent neurones, and that the after-depolarization was in fact an excitatory post-synaptic potential (e.p.s.p.). Dichter & Fischbach (1977) showed that the after-depolarization persisted following block of propagation of axonal action potentials by tetrodotoxin, and suggested an alternative explanation: that the after-depolarization is triggered by calcium entry during the action potential acting on an undefined conductance mechanism. In voltage-clamp studies on the calcium current of chick sensory neurones Dunlap & Fischbach (1981) recorded persistent inward tail currents following depolarizing voltage jumps, and suggested that these were the basis of the after-depolarization described by Dichter & Fischbach (1977).

Recent studies have shown the occurrence of several calcium-activated mechanisms in addition to the calcium-activated potassium conductance first described by Meech (1978). Non-selective cation-permeable channels activated by calcium occur in cardiac (Colquhoun, Neher, Reuter & Stevens, 1981), neuroblastoma (Yellen, 1982), and pancreatic acinar (Maruyama & Petersen, 1982) cell membranes. In addition a calcium-activated anion-permeable conductance mechanism has been described in *Xenopus* oocytes (Miledi, 1982; Barish, 1983; Miledi & Parker, 1984), salamander retina rod inner segments (Bader, Bertrand & Schwartz, 1982), mouse spinal cord neurones (Owen, Segal & Barker, 1984) and rat lacrimal gland cells (Marty, Tan & Trautmann, 1984). The results of voltage-clamp experiments presented in this paper suggest that the after-depolarization of mammalian sensory ganglion neurones results from activation of a calcium-dependent anion conductance which carries inward depolarizing current. A brief abstract of the result was presented to the Physiological Society (Mayer, 1985).

METHODS

Dorsal root ganglia were dissected from 1-day-old rat pups, dissociated, and grown in culture using standard techniques (Ransom, Neale, Henkart, Bullock & Nelson, 1977). Intracellular recording was performed on the stage of an inverted phase-contrast microscope, 2–11 weeks after plating using patch electrodes for whole-cell recording (Hamill, Marty, Neher, Sakmann & Sigworth, 1981), and an Axon Instruments discontinuous voltage-clamp amplifier.

Patch pipettes were fabricated from borosilicate glass using a two-stage process, and had resistances of 5–12 MΩ. This gave a series resistance larger than that typically used for whole-cell recording, but rundown of calcium currents due to intracellular dialysis appeared to occur slowly such that calcium currents and conductance mechanisms activated by calcium entry could be routinely studied for periods in excess of 30 min. Intracellular dialysis with caesium, as judged by block of outward potassium currents during brief depolarizing voltage jumps, took from between

10 and 200 s when recording from sensory neurones of somal diameter approximately 25 μm. Although net membrane currents of several nanoamperes were recorded during the present experiments, the use of a discontinuous voltage-clamp amplifier switching at approximately 10 kHz removed the limitations normally imposed by series resistance in voltage-clamp recording.

The technique used for establishing whole-cell recording was suggested by G. L. Westbrook, and is different from that described by Hamill *et al.* (1981). Pipettes were lowered onto cells during repetitive passage of hyperpolarizing current pulses 30 ms in duration and 100 pA in amplitude using the bridge-recording mode of the voltage-clamp amplifier. Contact with the cell was signalled by a small increase in pipette resistance; on application of suction a gigohm seal was formed and the current pulse was reduced to 10 pA. The actual seal resistance could not be accurately measured with this technique but was usually greater than 5 GΩ, as calculated from the electrotonic potential produced by 30 ms 10 pA current pulses (the time constant of such patch electrotonic potentials was in excess of 30–40 ms and hence the use of brief current pulses underestimated the seal resistance). Application of further suction established whole-cell recording, signalled by a fall in input resistance and appearance of a d.c. membrane potential.

The patch pipettes were filled with a solution containing (mM): 140, CsCl or KCl; 2, $MgCl_2$; 1·1, EGTA (pCa ~ 8); 10, HEPES titrated to pH 7·2 with KOH. Sucrose was used to adjust the osmolarity to 310 mosmol. KCl was used as the major internal salt in current-clamp experiments, while CsCl was used to block outward potassium currents in voltage-clamp experiments. The bathing medium, at room temperature (24–26 °C), contained (mM): 145, NaCl or NaBr; 4·8, KCl; 1, $MgCl_2$; 2·5, $CaCl_2$; 10, glucose; 10, HEPES; 0·01 mg Phenol Red/ml and was titrated to pH 7·3 with NaOH. In some experiments the bathing medium contained 0·2 mM-CsCl to block inward rectifier currents (Mayer & Westbrook, 1983). Test solutions of differing composition were applied by pressure from micropipettes (see Mayer & Westbrook, 1983, 1984 for details), or by perfusion at 5 ml/min using standard 35 mm tissue culture plates as the recording chamber. In voltage-clamp experiments 0·5–1·0 μM-tetrodotoxin (TTX) was used to block axonal sodium currents, which otherwise appeared as all or non-inward current spikes during depolarizing voltage jumps; in the majority of these experiments 2·5–10 mM-tetraethylammonium (TEA) bromide or chloride was added to the recording medium, to further suppress axonal potassium currents.

Test solutions containing $CdCl_2$ (0·2–1·0 mM) and $CoCl_2$ (2·0 mM), added directly to the bathing medium, were applied by pressure. The following test solutions were applied by perfusion: calcium-free solution, prepared by substituting $MgCl_2$ for $CaCl_2$; barium solution, prepared by substituting $BaCl_2$ for $CaCl_2$; sodium-free solution prepared by substituting TEA bromide for NaBr; low-chloride solution prepared by substituting mannitol for NaCl. The junction potential change produced by switching between these solutions (and measured with a patch pipette in the recording bath) was less than 2 mV and was not compensated for.

RESULTS

Spike after-potentials

The action potential of mouse and rat dorsal root ganglion neurones impaled with micro-electrodes containing potassium acetate is invariably followed by a hyperpolarizing after-potential. However, when patch electrodes filled with KCl were used for whole-cell recording, rat sensory neurones showed both hyperpolarizing and depolarizing after-potentials (Fig. 1). The resting potential, input resistance, action potential amplitude and half-width were similar in neurones with and without depolarizing after-potentials. In those neurones displaying a depolarizing after-potential an initial rapid phase of spike repolarization usually produced a hyperpolarizing undershoot of the membrane potential which appeared to be curtailed by development of a slowly rising depolarizing after-potential (Fig. 1). Such after-potentials had rise times of 10–20 ms, and peak amplitudes of 10–25 mV.

The amplitude and duration of the after-hyperpolarization recorded using patch electrodes appeared to be smaller than that observed using micro-electrode recording,

although no quantitative measurements were made to confirm this. It is possible that the use of patch electrodes containing EGTA helps to buffer calcium entry during the action potential, which would otherwise activate a calcium-dependent potassium conductance.

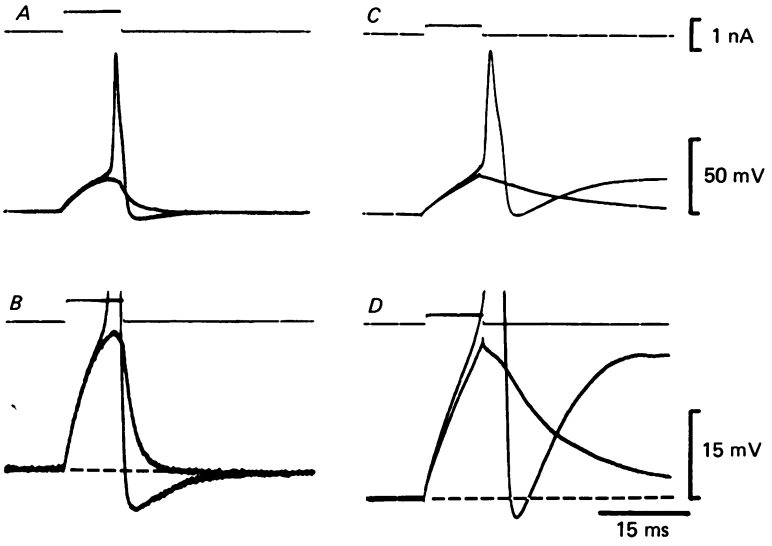

Fig. 1. Hyperpolarizing and depolarizing after-potentials recorded from two sensory ganglion neurones using patch pipettes filled with KCl for whole-cell recording. The records show two superimposed traces on threshold for responses evoked by current pulses 10 ms in duration. *A* and *B* were obtained from one neurone with a hyperpolarizing after-potential; note the relatively brief duration of the after-hyperpolarization shown at high gain in *B* (resting potential −58 mV). Responses from another neurone with a depolarizing after-potential are shown in *C* and *D* (resting potential −56 mV); note the initial hyperpolarizing undershoot preceding the slowly rising depolarizing after-potential in *D*. The bathing medium did not contain TEA or tetrodotoxin.

Single action potentials evoked at low frequencies produced depolarizing after-potentials that showed temporal summation. In those sensory neurones lacking rapid accommodation to depolarizing current pulses, the after-depolarization produced by single action potentials was capable of triggering burst responses consisting of a train of action potentials riding on the depolarizing after-potential (Fig. 2). Such burst responses were prevented by membrane potential hyperpolarization such that the depolarizing after-potential did not reach threshold for action potential generation. The amplitude and duration of the after-potential following burst responses was much larger than that evoked by single action potentials in the same neurone (Fig. 2), possibly due to cumulative calcium entry during trains of action potentials.

The amplitude of action potentials recorded during bursts triggered by depolarizing after-potentials decreased with time (Fig. 2), probably as a result of sodium current inactivation. In addition the membrane resistance, measured using brief hyperpolarizing current pulses, showed a large decrease during the after-depolarization, and it is possible that this also contributes to the fall in action potential amplitude.

Voltage clamp of the depolarizing after-potential

The conductance mechanism underlying the depolarizing after-potential evoked by single action potentials could be voltage clamped by electronically activating the clamp as the membrane potential returned to its resting value during the initial rapid phase of post-spike repolarization, revealing an inward current with slow activation

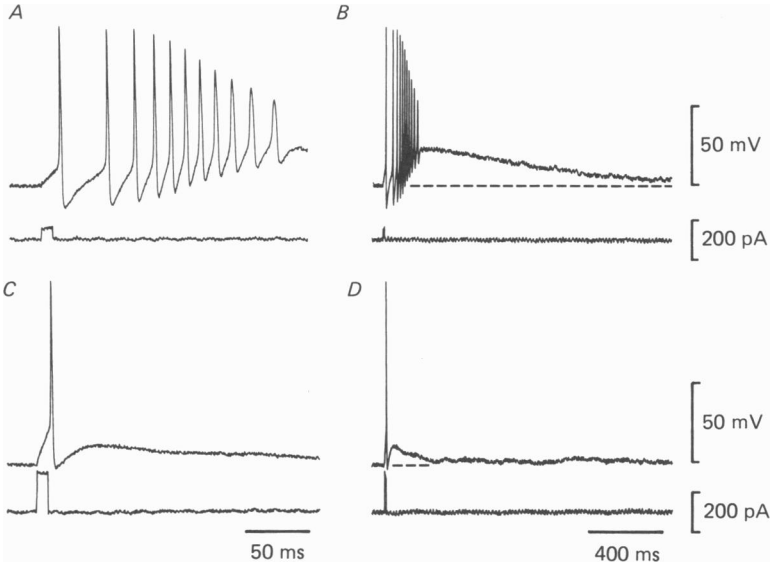

Fig. 2. Burst responses recorded from one sensory neurone displaying a depolarizing after-potential. *A* and *B* show responses evoked from the resting potential (−50 mV) by depolarizing current pulses 10 ms in duration and recorded at two different sweep speeds; note the increasing frequency of discharge during the initial phase of the response preceding the fall in action potential amplitude at the peak of the response. *C* and *D* were obtained at a membrane potential of −60 mV during injection of d.c. hyperpolarizing current to reveal the underlying depolarizing after-potential; note the difference in duration of the after-potentials triggered by burst responses (*B*) and single action potentials (*D*). The records were obtained using a KCl-filled pipette for whole-cell recording; the bathing medium did not contain TEA or tetrodotoxin.

and decay (Fig. 3*A*). Analysis of the underlying conductance mechanism was complicated by the simultaneous activation of calcium-dependent potassium current (for review see Meech, 1978) and to further study the properties of the slow inward current in isolation, brief depolarizing voltage jumps were used to activate the underlying conductance mechanism in sensory neurones which were loaded with CsCl and bathed in medium containing TTX to block sodium currents and TEA to block potassium currents. This protocol evoked inward calcium currents in all neurones. In addition, in thirty-one of sixty-eight cells, on repolarization to the resting potential, slowly decaying inward tail currents similar to those evoked by action potentials were also recorded (Fig. 3*B*).

Fig. 3*C* and *D* shows examples of currents evoked by depolarizing voltage jumps in two neurones, one with and one without a slow inward tail current. This tail

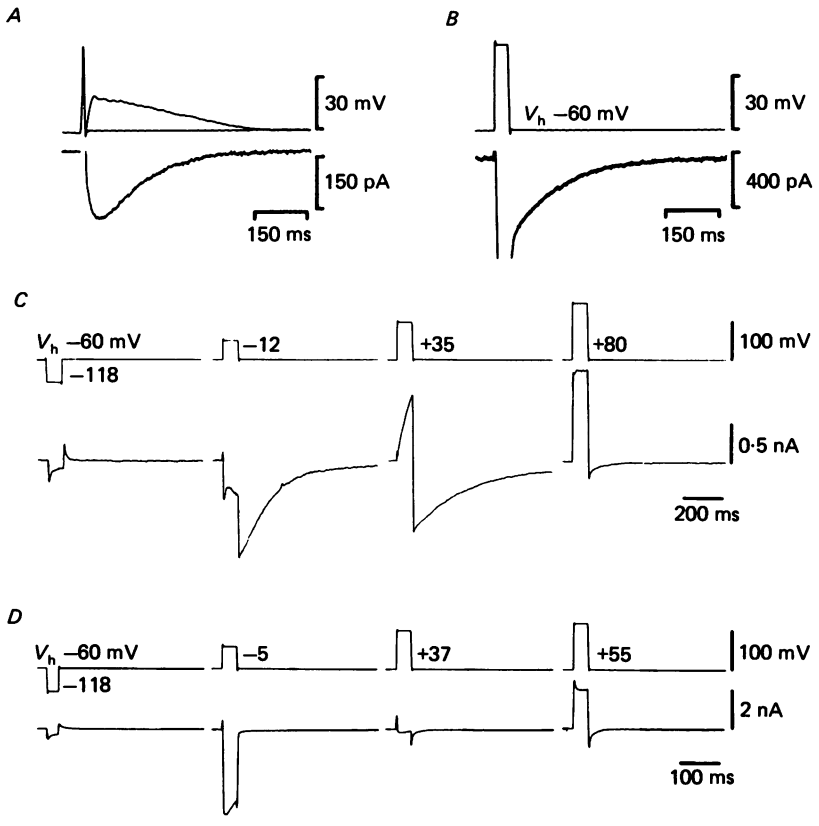

Fig. 3. Slowly decaying inward currents triggered by action potentials and depolarizing voltage jumps. *A* shows chart records of the membrane potential (upper traces) and clamp current (lower trace) obtained during voltage clamp of the depolarizing after-potential. Single action potentials were triggered by brief depolarizing current pulses, and the clamp electronically activated as the membrane potential repolarized to its resting value, before the slowly rising depolarizing after-potential developed. The voltage record shows two superimposed traces, one of the unclamped after-potential, and one during voltage clamp at −60 mV; the responses were recorded using a patch pipette containing KCl, in the absence of TEA and tetrodotoxin. The action potential amplitude is truncated by the frequency response of the chart recorder. *B* shows a slowly decaying inward current triggered by a depolarizing voltage jump from −60 to −12 mV and recorded from another cell using a patch pipette containing CsCl; during the voltage jump a net inward current occurred, the peak amplitude of which was truncated by the chart recorder. *C* and *D* show responses recorded from two sensory neurones during voltage jumps to various potentials from a holding potential (V_h) of −60 mV. *C* shows slow relaxations and prolonged tail currents due to the calcium-activated anion conductance described herein. *D* shows typical records from a neurone in which depolarization activated only a calcium current gating with rapid activation and deactivation kinetics. In these and subsequent voltage-clamp records the bathing medium contained TEA and tetrodotoxin, and CsCl was used in the patch pipettes unless otherwise noted.

current, as shown below, appears to result from activation of a calcium-dependent anion conductance, and for brevity will be referred to as $I_{Cl(Ca)}$. For both of the examples shown, depolarizing voltage jumps to potentials of around −10 mV produce net inward currents. In the one neurone with slow tail currents (Fig. 3*C*), the inward current recorded at −12 mV shows a slow inward relaxation, while further depolarization to +35 mV causes a slow outward relaxation of a net outward current. Since both intracellular and extracellular potassium-channel blockers were used in this experiment, it is probable that some conductance mechanism other than a voltage- or calcium-dependent potassium current underlies the time-dependent outward current seen in this neurone. On depolarization to +80 mV the outward current does not show time dependence and no slow inward tail current is recorded on repolarization to −60 mV; in contrast, jumps to −12 and +35 mV are followed by slow inward tail currents characteristic of $I_{Cl(Ca)}$.

For neurones lacking $I_{Cl(Ca)}$, depolarizing voltage jumps to around −10 mV produce net inward currents invariably accompanied by small outward relaxations (Fig. 3*D*), possibly due to voltage- or calcium-mediated inactivation of calcium conductance. This inward current is blocked by 0·2 mM-cadmium and has a similar voltage-dependent activation to calcium currents in other vertebrate neurones. For the example shown in Fig. 3*D*, on depolarization to approximately +35 mV, the outward leak current is balanced by an inward current, producing zero net membrane current with minimal time dependence during the voltage jump; further depolarization produces net outward current. In this and other neurones lacking $I_{Cl(Ca)}$ slow inward tail currents were not observed on repolarization to −60 mV following activation of calcium currents by depolarizing commands to a wide range of membrane potentials.

Fig. 4 shows examples of current–voltage plots from two sensory neurones, one with (*A*) and one without (*C*) $I_{Cl(Ca)}$, measured using voltage jumps 55 and 35 ms in duration. In both groups of cells peak inward current occurred around 0 mV: for cells with $I_{Cl(Ca)}$ the range was −10 to 0 mV (mean −4·1 ± 3·8 mV, $n = 12$); for cells without $I_{Cl(Ca)}$ the range was 0 to +10 mV (mean +4·0 ± 4·2 mV, $n = 5$). Depolarization beyond this potential produced *net* outward current at different potentials in the two groups of neurones: for those with $I_{Cl(Ca)}$ the membrane current measured using voltage jumps 30–60 ms in duration reversed polarity at −2 to +22 mV (mean +12·4 ± 12·4 mV, $n = 11$); for cells without $I_{Cl(Ca)}$ the membrane current reversed at +27 to +38 mV (mean +34·2 ± 4·3 mV, $n = 5$). This difference reflects activation of an outward current at membrane potentials depolarized to 0 mV in the subpopulation of sensory neurones with $I_{Cl(Ca)}$, even during voltage jumps of only 30–60 ms in duration (see Fig. 3). Longer-duration voltage jumps produced greater activation of time-dependent outward current in neurones with $I_{Cl(Ca)}$, and a hyperpolarizing shift in the potential at which the membrane current voltage plot intersected the voltage axis.

For those neurones with $I_{Cl(Ca)}$, plots of the slow inward tail current amplitude recorded at −60 mV as a function of membrane potential during the depolarizing prepulse were U shaped (Fig. 4*B*), with a peak between 0 and +5 mV (mean +3·12 ± 2·5 mV, $n = 16$), i.e. similar to the membrane potential at which peak inward calcium current is recorded (Fig. 4*B*). Depolarization to more positive membrane potentials strongly reduced the amplitude of the slow inward tail current. These

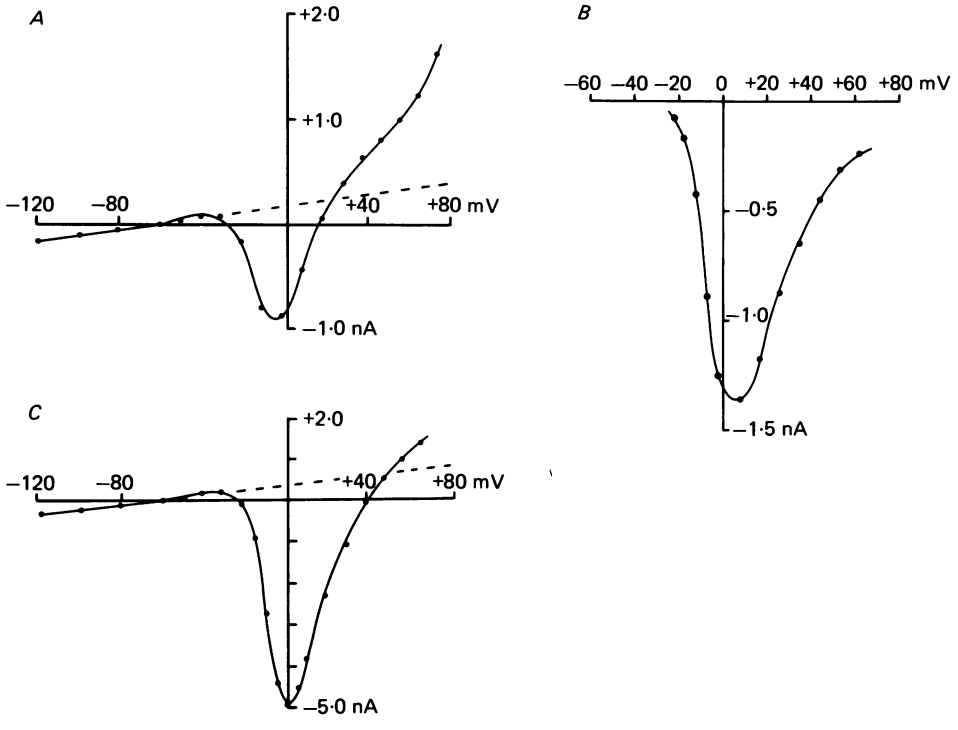

Fig. 4. Current–voltage and tail current availability plots. *A* shows the current–voltage relation of a sensory neurone showing slow relaxations similar to those illustrated in Fig. 3*C*, and recorded at the end of 55 ms voltage jumps from a holding potential of −60 mV. *B* shows a plot of the tail current amplitude measured 30 ms after repolarization to −60 mV, following depolarizing voltage jumps from a holding potential of −60 mV to the command potentials indicated on the *x* axis, and recorded from a neurone showing slowly decaying tail currents. *C* shows a current–voltage plot recorded from a neurone with only a calcium current, similar to that illustrated in Fig. 3*D*; measurements were made at the end of 35 ms duration voltage jumps from a holding potential of −60 mV. Dashed lines show extrapolated leak conductance; note the activation of outward current in *A* but not in *C* at membrane potentials positive to +20 mV.

results, and those shown in Figs. 2 and 3, suggest that $I_{Cl(Ca)}$ is triggered by calcium entry during action potentials and depolarizing voltage jumps. The conductance mechanism appears to be limited to a subpopulation of 46% of the cells studied in these experiments.

Calcium sensitivity of $I_{Cl(Ca)}$

The U-shaped availability curve shown in Fig. 4*B* suggests that calcium entry is required for activation of the conductance mechanism underlying $I_{Cl(Ca)}$. To examine directly the calcium dependence of $I_{Cl(Ca)}$ the extracellular medium was exchanged for one in which magnesium (2·5 mM) was substituted for calcium. In three cells this reversibly abolished both the slow inward and outward relaxations attributed to $I_{Cl(Ca)}$, resulting in a more linear current–voltage relation over the range −100 to +50 mV (Fig. 5). The slow inward tail currents attributed to $I_{Cl(Ca)}$ were also dramatically reduced in calcium-free solution (Fig. 5).

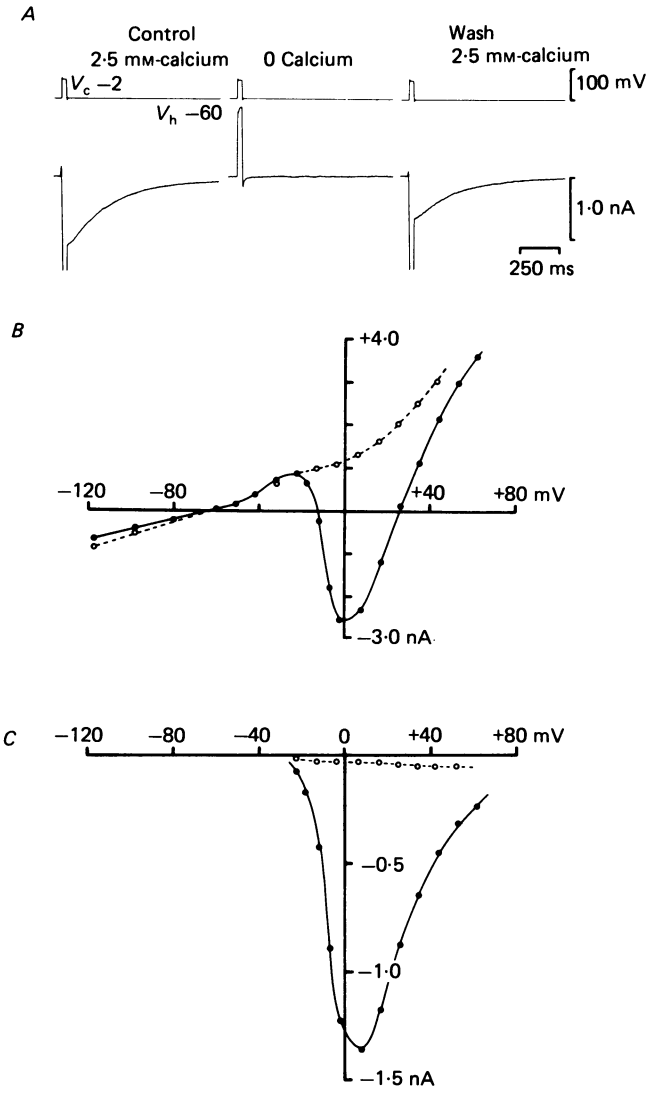

Fig. 5. Calcium dependence of the slow inward tail current. *A* shows raw data from a single neurone during perfusion with nominally calcium-free solution. Depolarizing voltage jumps to a command potential (V_c) of −2 mV for 30 ms were used to trigger inward calcium currents (off-scale here) which were followed by slowly decaying inward tail currents on return to −60 mV; on removal of extracellular calcium both the inward calcium current and slow tail current were reversibly abolished (the trace labelled 0 calcium was recorded 140 s after perfusing the plate with calcium-free medium). *B* shows current–voltage plots from one sensory neurone recorded in normal medium containing 2·5 mM-calcium (●) and in calcium-free medium (○); the holding potential (V_h) was −60 mV and the current–voltage relation was measured at the end of 30 ms voltage jumps. Note the loss of net inward current and the fall in slope conductance at positive membrane potentials that occurs in calcium-free medium. *C* shows a plot of the slow tail current amplitude measured 30 ms following repolarization to −60 mV *versus* membrane potential during the depolarizing pre-pulse used to activate the slow tail current (●). In calcium-free medium the tail current is greatly reduced at all membrane potentials (○).

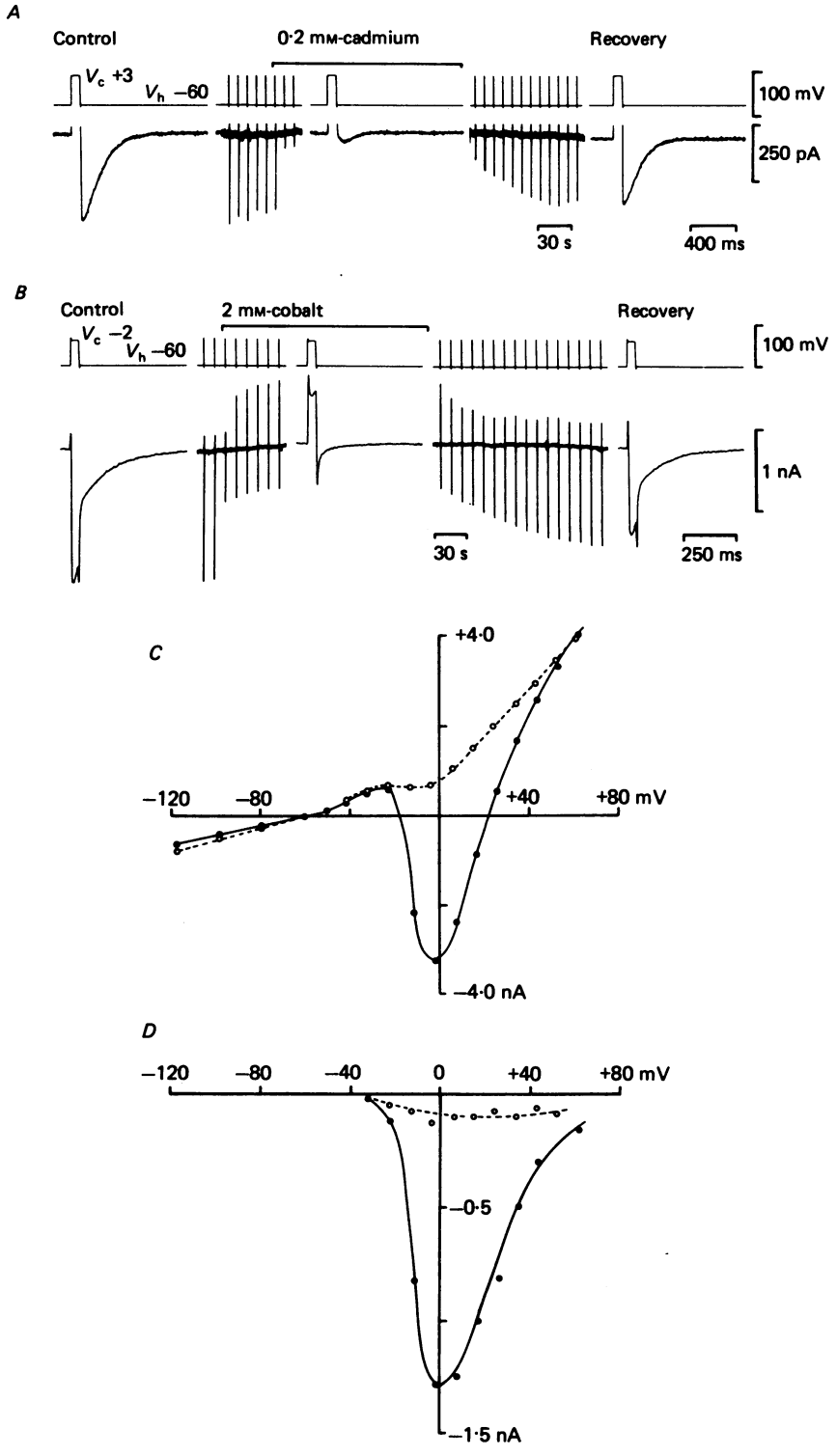

Fig. 6. For legend see opposite.

A similar, and reversible, depression of the slow inward tail currents and relaxations attributed to activation of $I_{Cl(Ca)}$ occurred during pressure application of the calcium-channel blockers cadmium (0·2–1 mM, $n = 5$) or cobalt (2 mM, $n = 2$) (Fig. 6). In the presence of these calcium-channel blockers, the membrane current–voltage plot over the range -100 to $+50$ mV was more linear (Fig. 6), providing further evidence that $I_{Cl(Ca)}$ is largely dependent upon a prior, or simultaneous calcium entry.

Activation of transmitter release (Augustine & Eckert, 1984), calcium-dependent potassium current (Gormann & Herman, 1979) and calmodulin (Teo & Wang, 1973) are calcium-specific processes for which barium cannot substitute. To examine the effect of barium on the slow inward tail currents attributed to $I_{Cl(Ca)}$ the bathing medium was exchanged for one in which 2·5 mM-$BaCl_2$ was substituted for $CaCl_2$. In three neurones this reversibly abolished $I_{Cl(Ca)}$ tail currents. In each of these experiments the inward current activated on stepping to 0 mV, i.e. close to the reversal potential for $I_{Cl(Ca)}$, was also reduced on replacing calcium by barium. This was unexpected since there are many studies showing that barium passes through calcium channels, and may in fact be a better charge carrier than calcium (e.g. Fenwick, Marty & Neher, 1982). It is possible that incomplete exchange of barium for calcium during perfusion with barium-substituted solutions produced an extreme example of anomalous mole fraction behaviour and reduction of inward current through calcium channels (for example see Almers & McClesky, 1984).

Membrane conductance changes and reversal potential of $I_{Cl(Ca)}$

To estimate changes in membrane conductance during the slow inward tail current, brief hyperpolarizing voltage jumps were superimposed on the voltage-clamp protocol used to activate $I_{Cl(Ca)}$ (cf. DiFrancesco, 1981). To be of use this technique requires that the instantaneous current–voltage relation be linear (see Fig. 8) and that, if present, time- and voltage-dependent changes in conductance occur with slow kinetics (see Figs. 11 and 12 and Marty *et al.* 1984). This procedure revealed conductance increases of 12–54 nS (mean $31 \pm 13·9$, $n = 8$). A constant relation between the amplitude of the inward current and the increase in membrane conductance (Fig. 7) suggests that the driving force remains constant during decay of the tail current. Thus, accumulation or depletion of ions in unstirred layers

Fig. 6. Reversible antagonism of slow inward tail currents by calcium-channel blockers. *A* shows block by 0·2 mM-cadmium of inward tail currents activated by depolarizing voltage jumps to a command potential (V_c) of +3 mV for 80 ms. In this experiment the patch electrode was filled with KCl and the bathing medium did not contain TEA or tetrodotoxin; the outward current recorded during the voltage jump is clipped by the chart recorder. *B* shows reversible block by 2 mM-cobalt of the inward calcium current and slow tail current triggered by 35 ms voltage jumps to -2 mV. *C* shows a current–voltage plot recorded at the end of 40 ms voltage jumps from a holding potential of -60 mV before (●) and during application of 2 mM-cobalt (○). Note the loss of net inward current and the fall in slope conductance at positive membrane potentials on perfusion with cobalt. *D* shows a plot of the inward tail current amplitude recorded 30 ms following repolarization to -60 mV *versus* the membrane potential during depolarizing voltage commands to between -40 and +60 mV; the tail current is greatly reduced by cobalt at all membrane potentials; (●) control; (○) 2 mM-cobalt.

adjacent to the sensory neurone membrane do not appear to interfere with analysis of the conductance mechanism, despite its relatively prolonged time course.

To estimate the reversal potential of the slow inward current a two-step voltage-clamp protocol was used (Fig. 8). In six neurones, the current–voltage relation at the peak of the slow inward tail current was linear over the potential range −100 to

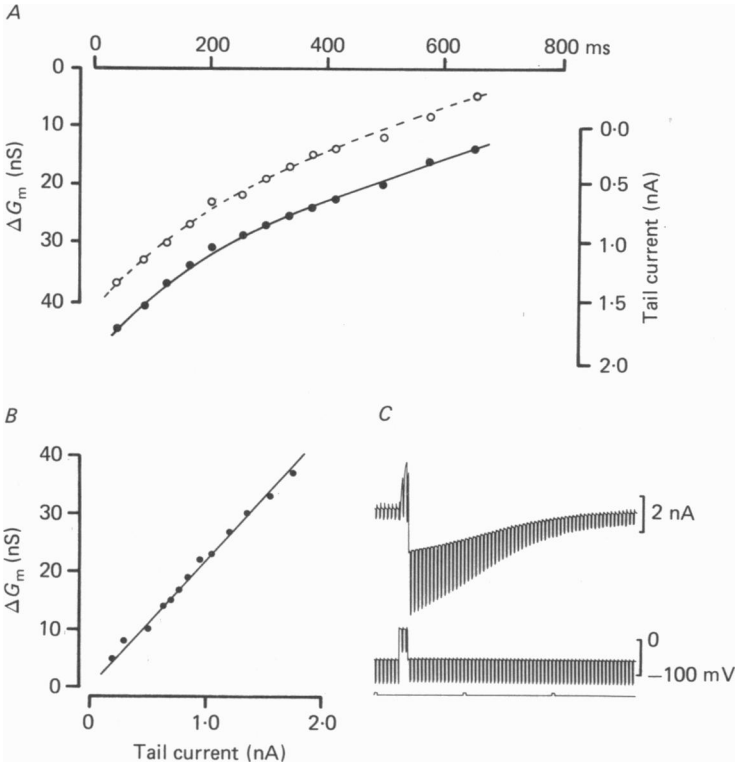

Fig. 7. Membrane conductance (G_m) is increased during the slowly decaying tail current. *A* shows the tail current amplitude (●) and accompanying increase in membrane conductance (○) plotted against time following return to −60 mV, after a depolarizing voltage jump to +25 mV for 100 ms was used to activate the slow tail current conductance mechanism. Membrane conductance was measured using 60 mV hyperpolarizing voltage jumps 10 ms in duration. *B* shows a correlation plot of the increase in membrane conductance *versus* tail current amplitude. *C* shows the tail current used to generate this analysis.

−40 mV, giving extrapolated reversal potentials of −27 to −1 mV (mean −12 ± 9·6 mV). Direct reversal of the tail current could not be demonstrated using this protocol, since further depolarization during the second pulse activated the mechanism producing $I_{Cl(Ca)}$ (see Figs. 3 and 4). However, by using brief voltage jumps of variable amplitude and polarity during either the tail current or the depolarizing pre-pulse used to activate $I_{Cl(Ca)}$ a more direct estimate of reversal was possible (Fig. 8*C*); this procedure gave similar estimates of the reversal potential to that recorded using twin pulses.

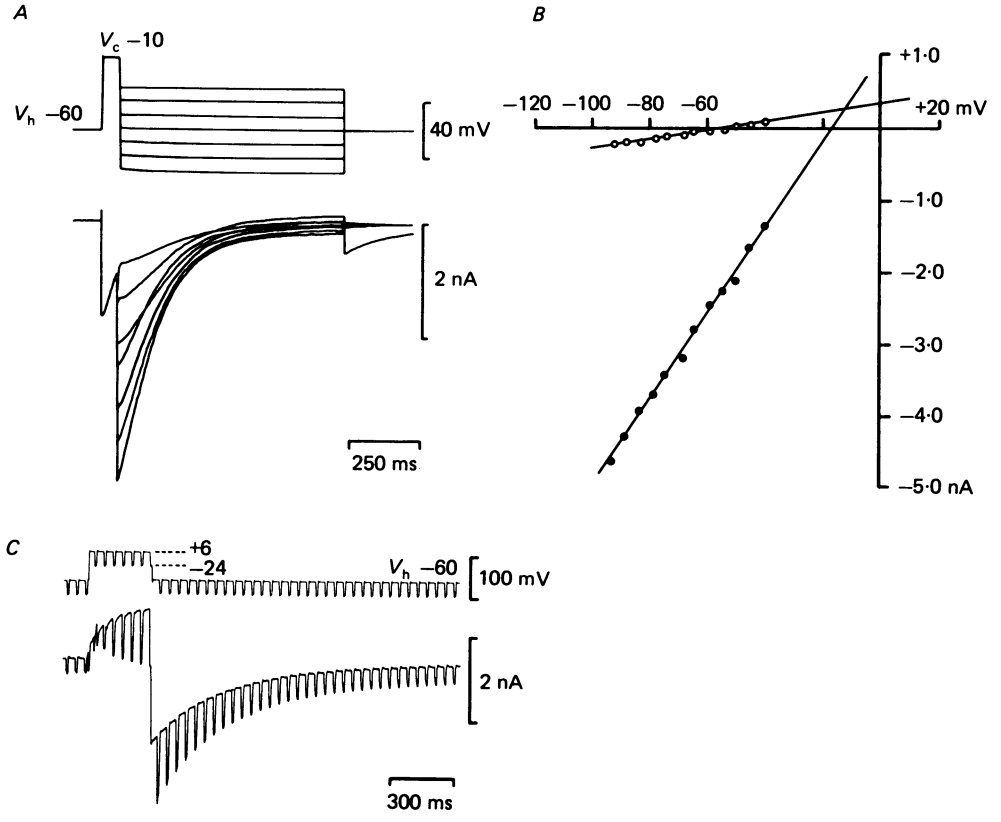

Fig. 8. Current–voltage relation of the slow inward current. *A* shows the clamp protocol (membrane potential upper trace) used to estimate the reversal potential of the slow inward tail current activated by a depolarizing pre-pulse (lower trace); the decay of the tail current becomes faster with hyperpolarization. *B* shows a plot of the tail current amplitude recorded 20 ms (●) and 800 ms (○) after the voltage jump to the test potential, i.e. at the peak of the tail current and after the current has decayed. At the peak of the inward tail current the membrane current–voltage relation is linear with a slope conductance of 60 nS; at 800 ms the membrane current–voltage relation has a slope conductance of 6·3 nS. Intersection of the current–voltage relations occurs at −12 mV, the extrapolated reversal potential of the tail current. In this experiment the bathing medium contained 0·2 mM-CsCl to block inward rectification. *C* shows raw data from another neurone showing slow activation of the mechanism underlying the inward tail current. A 300 ms voltage jump to +6 mV was used to activate the conductance; during this period hyperpolarizing voltage jumps 10 ms in duration were used to measure the membrane conductance. At +6 mV activation of the conductance mechanism is seen as a slow outward relaxation; the envelope of the conductance testing pulses at −24 mV is seen as a slow inward relaxation. Such envelope experiments provide an alternative method of estimating the reversal potential of the conductance underlying the slow relaxation.

Ionic dependence of $I_{Cl(Ca)}$

Slow inward current tails dependent on prior calcium entry could result from activation of non-specific cation-permeable channels of the type described by Colquhoun *et al* (1981); this mechanism appears to operate in chromaffin cells (Fenwick *et al.* 1982). To test for this possibility in sensory neurones TEA ions, which should be too large to pass through the non-specific channel, were used as a substitute for sodium (Fig. 9). This procedure slowed decay of the inward tail currents activated by depolarizing commands, and caused a biphasic change in amplitude; on changing to sodium-free solution, the tail current showed a transient increase in amplitude before starting to irreversibly decline. This does not support a role for sodium as a charge carrier for the slow inward current, since replacement of sodium by TEA should greatly reduce the driving force for inward current.

By normalizing the tail current amplitude with respect to the initial inward calcium current recorded during a depolarizing pre-pulse it was possible to use a twin-pulse protocol to estimate the reversal potential for the slow inward tail current despite the non-stationarity imposed by rundown of the calcium current in sodium-free solution (Fig. 9). Using this procedure in three neurones there was no change in the reversal potential change for $I_{Cl(Ca)}$ on substituting TEA for sodium (Fig. 9).

The reversal potential of $I_{Cl(Ca)}$, around -10 mV under the present experimental conditions, is hyperpolarized to the reversal potential expected for a calcium current. The experimentally measured potential (approximately $+40$ mV) at which membrane currents reverse to net outward currents in those neurones in which $I_{Cl(Ca)}$ is absent (see Fig. 4), although considerably depolarized to -10 mV (the reversal potential of $I_{Cl(Ca)}$) is likely to underestimate the true calcium reversal potential if caesium carries outward current through calcium channels (Lee & Tsien, 1984). Thus, on the basis of reversal potential measurements the slow inward tail currents recorded in these experiments do not appear to result from activation of a calcium current gating with slow kinetics (cf. MacDonald & Schneiderman, 1984).

Since the inward tail currents were only recorded when using patch electrodes filled with solutions of chloride salts it is probable that an efflux of chloride ions via a calcium-activated anion-permeable channel generates $I_{Cl(Ca)}$. To test this directly mannitol was used as substitute for NaCl in the extracellular medium. In these experiments the tail current amplitude was dramatically increased on switching to low-chloride solution (Fig. 10), presumably as a result of an increase in driving force for chloride efflux. A twin-pulse protocol was used in an attempt to estimate the tail current reversal potential, but apparent collapse of the increased chloride ion gradient during the course of these experiments made it impossible to accurately calculate reversal potential shifts. Single-channel recording experiments using isolated patches would considerably help in determining the selectivity of the ionic mechanism of $I_{Cl(Ca)}$, but taken together the present results provide no evidence for a cation-permeable mechanism, and suggest that $I_{Cl(Ca)}$ is an anion conductance. The reversal potential of $I_{Cl(Ca)}$ was similar in media made with NaCl and NaBr, suggesting that the conductance mechanism does not discriminate between Cl^- and Br^-.

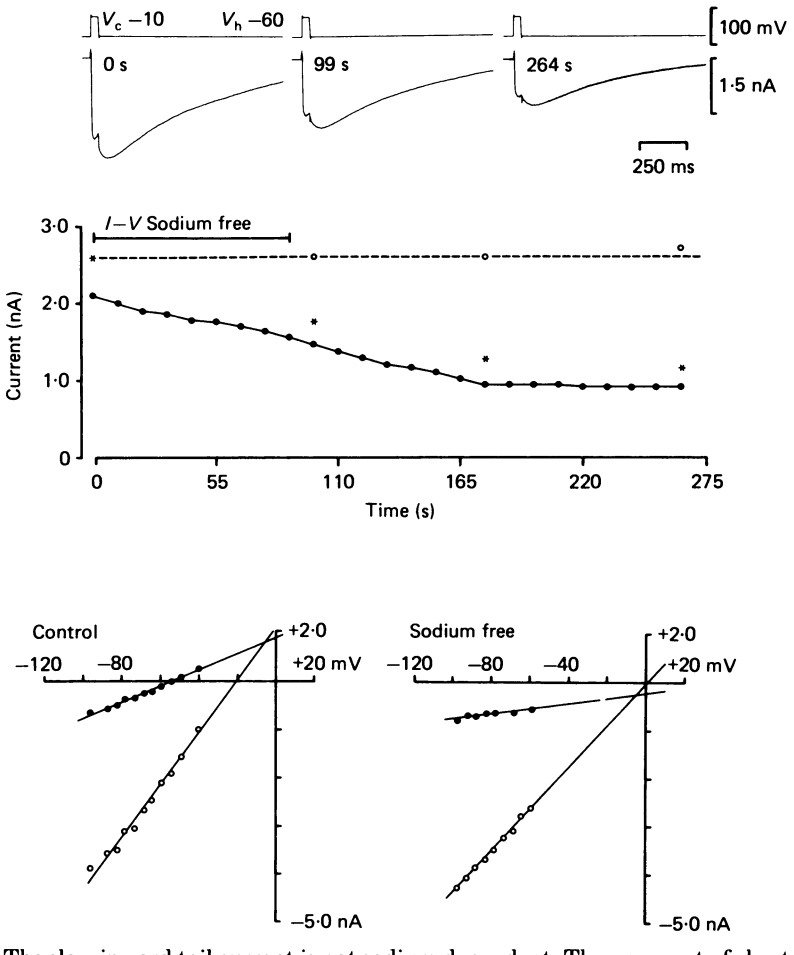

Fig. 9. The slow inward tail current is not sodium dependent. The upper set of chart traces show currents evoked by 40 ms depolarizing voltage jumps from −60 to −10 mV and recorded after perfusing the plate with sodium-free solution, using TEA bromide as a replacement for NaBr. The traces were recorded at the start of a twin-pulse protocol used to estimate the tail current reversal potential (0 s), and at 99 and 264 s intervals thereafter. After changing to sodium-free solution the inward calcium current triggered during the depolarizing voltage jump showed rundown. A plot of the calcium current amplitude (●) *versus* time is shown below. At time 0, 99, 176 and 264 s the second voltage jump during the twin-pulse protocol was to −60 mV and comparison of the tail current amplitude recorded at this potential (*) also showed rundown. The dashed line shows the tail current amplitude assuming stationarity from the value recorded at time 0; by scaling the amplitude of the tail current with respect to the initial calcium current it was possible to construct current–voltage plots even during rundown of the conductance mechanism. This approach is justified since the re-scaled tail currents (○) recorded at −60 mV various times after the onset of rundown fall on the line expected for stationarity. The lower set of current–voltage plots were recorded before and after perfusion with sodium-free solution, as shown in Fig. 8. The extrapolated reversal potential, −5 mV, does not change on replacement of sodium by TEA.

Activation and deactivation kinetics of $I_{Cl(Ca)}$

During depolarizing voltage jumps, the membrane current showed slow relaxations due to activation of a conductance mechanism with a reversal potential similar to that of $I_{Cl(Ca)}$ (Fig. 8). To study the activation kinetics of $I_{Cl(Ca)}$ directly, envelope experiments were performed and the inward tail current amplitude recorded on

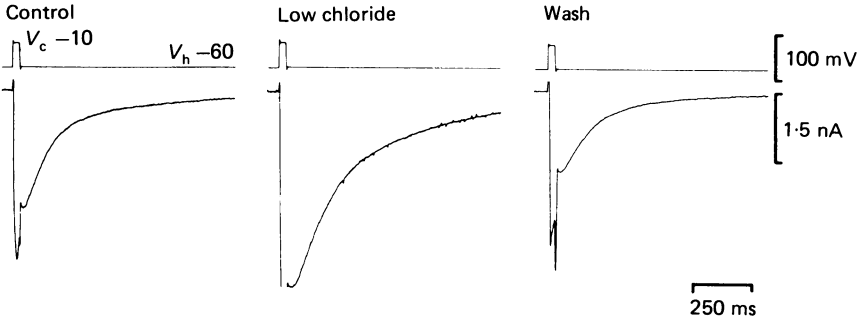

Fig. 10. Slow inward tail current amplitude shows chloride dependence. The chart traces show currents evoked by 30 ms voltage jumps from a holding potential (V_h) of −60 mV to a command potential (V_c) of −10 mV and recorded before, during and after perfusion with a low-chloride solution, prepared by substituting mannitol for NaCl (total Cl^-/Br^- change from 162 to 21 mM). The inward tail current reversibly increases in amplitude on reduction of the extracellular Cl^- concentration. The trace labelled low chloride was recorded 27 s after switching to medium containing 21 mM-permeable anion; at the perfusion rate used in this experiment this allowed for exchange of approximately two bath volumes.

repolarization to −60 mV plotted as a function of the duration of a depolarizing pre-pulse (Fig. 11). Activation of $I_{Cl(Ca)}$ at −10 to +8 mV was described by a single exponential function of time constant 36–155 ms (mean 94±47 ms, $n = 5$). However, in each of these neurones the decay of the tail current became complex and non-exponential as the duration of the pre-pulse was increased such that plots of the tail current integral as a function of pre-pulse duration showed no clear approach to a maximum, in contrast to the exponential growth to a maximum of the initial tail current amplitude (Fig. 11).

During prolonged depolarizing voltage jumps $I_{Cl(Ca)}$ did not appear to show appreciable inactivation. On repolarization to membrane potentials hyperpolarized to the activation threshold for $I_{Cl(Ca)}$ the tail current decay kinetics showed both voltage and use dependence (Fig. 12). At −60 mV, tail currents activated by depolarizing pre-pulses of duration 10–60 ms decayed as single exponential functions of time constant 141–272 ms (mean 208±55, $n = 5$). However, the decay time constant increased as a function of the duration of the pre-pulse, and in addition the tail current kinetics became more complex (Fig. 12*A* and *B*), and were no longer described by single exponential functions. In several experiments the tail currents evoked by action potentials or short depolarizing pre-pulses (for example see Fig. 9) showed an initial growth phase before starting to decay. This further complicated kinetic analysis. Such results suggest that for pre-pulse durations in excess of 60 ms,

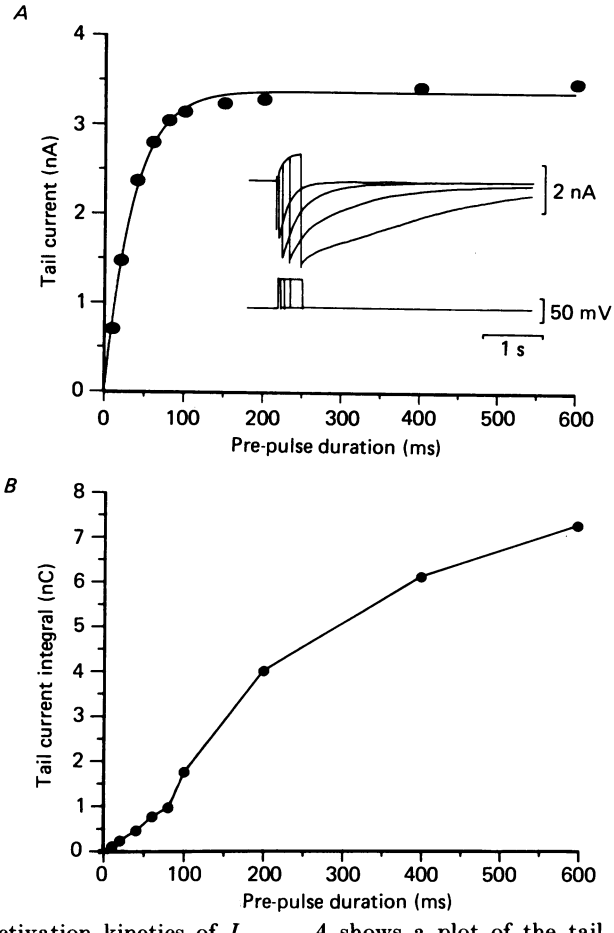

Fig. 11. Activation kinetics of $I_{Cl(Ca)}$. *A* shows a plot of the tail current amplitude measured 20 ms after repolarization to −60 mV *versus* the duration of a depolarizing pre-pulse to −2 mV. The continuous line is a single exponential best fit to the raw data with a time constant of 36 ms. The tail current approaches a maximum amplitude after pre-pulses 100 ms in duration. The inset shows tracings of raw data used for this analysis. In contrast *B* shows a plot of the integral of the tail current *versus* the duration of the depolarizing pre-pulse for the same raw data used to measure the time constant of activation shown in *A*. The integral continues to increase as the pre-pulse duration increases from 100 to 600 ms in duration and shows no approach to a maximum value over the same time period at which the tail current peak amplitude saturates.

decay of the tail current is determined by homoeostatic mechanisms controlling intracellular calcium activity. The results presented below, and those obtained by Marty *et al.* (1984) in studies on lacrimal gland cells, suggest that $I_{Cl(Ca)}$ also shows voltage-dependent changes in conductance.

Voltage dependence of the tail current kinetics was studied using a twin-pulse protocol with a short-duration pre-pulse, such that the decays were reasonably well described by single exponential functions. Using this approach in six cells the tail current relaxation became faster with hyperpolarization over the range −40 to −100 mV (Fig. 12). In five cells the decay time constant of $I_{Cl(Ca)}$ behaved as an

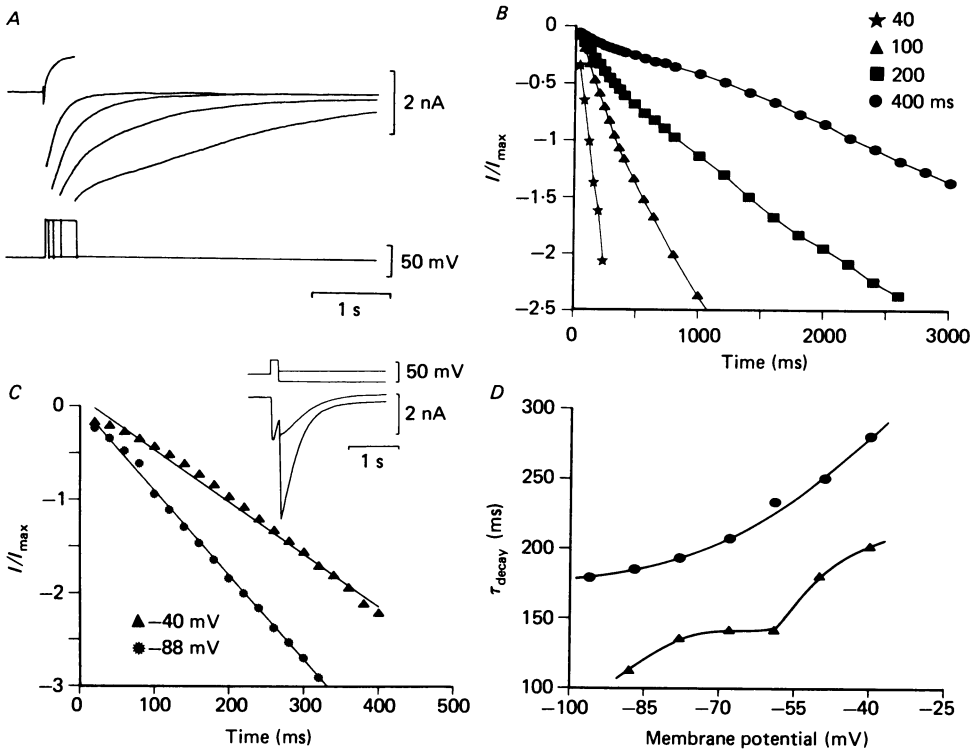

Fig. 12. Deactivation kinetics of $I_{Cl(Ca)}$. *A* shows raw data from an experiment in which the tail current decay at −60 mV was measured as a function of the duration of a depolarizing pre-pulse to −2 mV; note the exponential growth of the initial (i.e. peak) tail current envelope and the slowing of the tail current decay with increasing duration of the pre-pulse. *B* shows decay of the tail currents (I/I_{max}) illustrated in *A* as semilog plots *versus* time. Lines through the data points were fitted by interpolation; after pre-pulses of 200 and 400 ms duration the tail current decay is clearly not described by a single exponential function. *C* shows semilog plots of the decay of tail currents recorded at −40 and −88 mV in another neurone after a depolarizing pre-pulse to −10 mV for 60 ms. The decay is well described by a single exponential function of time constant 112 ms at −88 mV and 201 ms at −40 mV; the inset shows tracings of the raw data used for this analysis. *D* shows plots of the tail current decay time constant *versus* membrane potential for another two neurones; for one the decay time constant changes as an approximately exponential function of membrane potential (●), increasing e-fold per 118 mV depolarization (non-linear least-square fit to data), from 179 ms at −96 mV to 280 ms at −40 mV. For the second set of data shown in *D* the time constant of decay (▲) increases with depolarization but is not a simple exponential function of membrane potential; the reason for such behaviour is unclear.

approximately exponential function of membrane potential increasing on average e-fold per 120 mV depolarization over the range −100 to −40 mV (Fig. 12*D*). In lacrimal gland cells the calcium-activated chloride conductance increases e-fold per 106 mV depolarization (Marty *et al.* 1984). Such voltage dependence of the tail current kinetics appears to result from a genuine effect of membrane potential on gating; single-channel recording experiments in lacrimal gland cells exposed to the calcium

inophore A23187 clearly show voltage dependence of calcium-activated chloride channels (Marty *et al.* 1984). However, in lacrimal gland cells, the tail current decay time constant *increases* with hyperpolarization in contrast to the results described here. For the example shown in Fig. 8 the tail current kinetics were more complex, and the currents recorded at -50 and -60 mV show cross-over, reflecting an inflexion in the τ_{decay} – voltage plot for this neurone (Fig. 12*D*).

The complex nature of the kinetics of activation and inactivation of $I_{Cl(Ca)}$ may be a consequence of the presence of multiple mechanisms for regulation of intracellular free-calcium activity. In addition, release of calcium from intracellular stores may also activate $I_{Cl(Ca)}$ (see Neering & McBurney, 1984). In sensory neurones exposure to sodium-free solution prolonged the decay of $I_{Cl(Ca)}$, possibly as a result of reduced sodium–calcium exchange and a consequent increase in the duration of the intracellular calcium transient, suggesting that the slow time course of $I_{Cl(Ca)}$ may in part be limited by calcium sequestration.

DISCUSSION

Dissociated cultures of neurones from embryonic dorsal root ganglia have been useful in analysing the physiological properties of vertebrate sensory neurones, reflecting the ease with which voltage-clamp recording can be performed in this preparation. The present experiments strongly suggest that a population of mammalian sensory neurones have a calcium-activated anion-permeable conductance mechanism similar to that recently described in photoreceptors (Bader *et al.* 1982), spinal cord neurones (Owen *et al.* 1984) and lacrimal gland cells (Marty *et al.* 1984). Sensory ganglia contain a variety of cell types, and it is perhaps not surprising that not all of the neurones studied in these experiments generated depolarizing after-potentials. Further experiments are required to determine other differences between the two populations of neurones described here.

In studies on sensory neurones in acutely isolated preparations from adult animals depolarizing spike after-potentials were not reported (Ito, 1957, 1959; Gorke & Pierau, 1980) and it is unclear whether such potentials occur *in vivo*. In the present experiments, performed using patch electrodes for whole-cell recording, chloride loading raised the chloride equilibrium potential (E_{Cl}) to an artificially depolarized value, such that depolarizing after-potentials were easily detected. Under physiological conditions an inward-directed chloride pump does raise the intracellular chloride activity of sensory neurones above that expected for a passive distribution such that E_{Cl} lies between -22 mV (Gallagher, Higashi & Nishi, 1978) and -34 to -37 mV (Deschenes, Feltz & Lamour, 1976). Thus at the resting potential $I_{Cl(Ca)}$ could still generate inward depolarizing current, though of smaller amplitude than that recorded in the present experiments. In other studies on cultured sensory neurones in which spike after-depolarizations have been recorded (Crain, 1956, 1971; Neering & McBurney, 1984) KCl-filled micro-electrodes were used for intracellular recording, and it is unclear to what extent chloride loading occurred in these experiments.

It is of interest that depolarizing after-potentials were not observed in rat sensory neurones grown in culture and impaled with acetate-filled micro-electrodes (unpub-

lished observations). It is possible that acetate interferes with chloride fluxes (cf. Allen, Eccles, Nicoll, Oshima & Rubia, 1977), or alternatively that in these experiments E_{Cl} was close to the resting potential (cf. Choi & Fischbach, 1981). The interpretation of such current-clamp experiments is complicated since activation of a calcium-dependent potassium conductance (which appears to be expressed in a variety of cells), would tend to oppose any depolarizing action of an inward chloride current. Thus the shape and polarity of spike after-potentials will depend on the relative degree of activation, and difference in driving force for these two potentially opposing conductance mechanisms.

Recent studies on chick sensory neurones suggest the occurrence of several calcium currents (Nowycky, Fox & Tsien, 1984). In the present experiments the membrane potential was held at −60 mV between voltage jumps thus inactivating the transient calcium current; further experiments using a wider range of voltage protocols are required to determine if calcium currents other than the sustained non-inactivating conductance can contribute to the intracellular calcium transient activating $I_{Cl(Ca)}$.

The present experiments raise questions about the time course of intracellular calcium transients following action potentials and depolarizing voltage jumps. The slow rate of rise of the depolarizing spike after-potential can be accounted for by the slow activation kinetics of $I_{Cl(Ca)}$. The long duration of the spike after-depolarization recorded in the absence of potassium-channel blockade (see Figs. 1–3) suggests that the intracellular calcium activity is raised for around 100–400 ms following calcium entry during a single action potential, but it is possible that the slow deactivation kinetics of $I_{Cl(Ca)}$ also contributes to the slow decay of the after-potential. At −60 mV $I_{Cl(Ca)}$ decayed with a time constant of approximately 200 ms, similar to that reported by Marty *et al.* (1984) for the voltage-dependent deactivation of calcium-activated chloride current in lacrimal gland cells. In sensory neurones under voltage clamp, the decay time constant and integral of the slow inward tail current increases continuously with the duration of the depolarizing pre-pulse used to trigger calcium entry (see Fig. 12), suggesting that for larger calcium transients sequestration mechanisms may be the rate-limiting factor determining recovery to resting levels of calcium activity and consequent decay of $I_{Cl(Ca)}$.

Optical methods for direct measurement of calcium activity in the cytoplasm of sympathetic (Smith, MacDermott & Weight, 1983) and sensory (Neering & McBurney, 1984) ganglion neurones also show the calcium transient to decay with relatively slow kinetics; e.g. Neering & McBurney report a decay time constant of 100–200 ms for the increase in aequorin fluorescence activated by action potentials of width approximately 100 ms in the presence of 20 mM-TEA. Smith *et al.* (1983) used 5 s trains of action potentials to generate calcium transients, detected with Arsenazo III, which decay with a time constant of around 2 s. In squid giant synapses, the calcium transient triggered by single action potentials recorded under physiological conditions also persists for several hundred milliseconds (Miledi & Parker, 1981). In addition the kinetics of recovery from calcium-mediated inactivation of calcium current also suggest slow redistribution of intracellular calcium (Tillotson & Horn, 1978; Plant & Standen, 1981).

In some of the experiments described here the slow inward tail current showed complex kinetics with an initial growth phase preceding onset of decay (e.g. Fig. 9).

Although it is possible that simultaneous decay of an outward current caused an *apparent* growth phase of the inward tail current, the present experiments were performed using both intracellular and extracellular potassium-channel blockers, and inward tail currents were measured close to the potassium equilibrium potential (E_K). Thus it is possible that release of calcium from endoplasmic reticulum may occur following depolarization or calcium entry through the cell surface membrane, and that this may account for the initial growth of the inward tail current. It is of interest that during caffeine-triggered release of calcium from intracellular stores sensory neurones impaled with KCl-filled micro-electrodes do depolarize (Neering & McBurney, 1984), suggesting activation of $I_{Cl(Ca)}$.

The present qualitative description of a calcium-activated anion conductance in sensory neurones helps to explain the generation of the depolarizing after-potential first observed by Crain (1956). The kinetics of this conductance are complex, in part reflecting the nature of calcium regulation in sensory neurones. Further analysis of this mechanism will require the use of isolated membrane patches for study of the unitary conductance in experiments where both calcium activity and voltage can be controlled, and further knowledge of the mechanisms by which intracellular calcium activity is regulated.

The experimental work was performed at St. George's Hospital during tenure of a Beit Memorial fellowship, and was supported in part by M.R.C. grant G 8217750 N, and the Central Research Fund of the University of London. I thank Professor J. S. Kelly for the use of laboratory facilities, Bob Russell for preparing and maintaining the cultures, and Drs G. L. Westbrook and P. G. Nelson for their criticism of the manuscript.

REFERENCES

ALLEN, G. I., ECCLES, J. C., NICOLL, R. A., OSHIMA, T. & RUBIA, F. J. (1977). The ionic mechanisms concerned in generating the i.p.s.p.s of hippocampal neurones. *Proceedings of the Royal Society* B **198**, 363–384.

ALMERS, W. & MCCLESKEY, E. W. (1984). Non-selective conductance in calcium channels of frog muscle: calcium selectivity in a single-file pore. *Journal of Physiology* **353**, 585–606.

AUGUSTINE, G. J. & ECKERT, R. (1984). Divalent cations differentially support transmitter release at the squid giant synapse. *Journal of Physiology* **346**, 257–271.

BADER, C. R., BERTRAND, D. & SCHWARTZ, E. A. (1982). Voltage-activated and calcium-activated currents studied in solitary rod inner segments from the salamander retina. *Journal of Physiology* **331**, 253–284.

BARISH, M. E. (1983). A transient calcium-dependent chloride current in the immature *Xenopus* oocyte. *Journal of Physiology* **342**, 309–325.

CHOI, D. W. & FISCHBACH, G. D. (1981). GABA conductance of chick spinal cord and dorsal root ganglion neurons in cell culture. *Journal of Neurophysiology* **45**, 605–620.

COLQUHOUN, D., NEHER, E., REUTER, H. & STEVENS, C. F. (1981). Inward current channels activated by intracellular Ca in cultured cardiac cells. *Nature* **294**, 752–754.

CRAIN, S. M. (1956). Resting and action potentials of cultured chick embryo spinal ganglion cells. *Journal of Comparative Neurology* **104**, 285–330.

CRAIN, S. M. (1971). Intracellular recordings suggesting synaptic functions in chick embryo spinal sensory ganglion cells isolated *in vitro*. *Brain Research* **26**, 188–191.

DESCHENES, M., FELTZ, P. & LAMOUR, Y. (1976). A model for an estimate of the ionic basis of presynaptic inhibition: an intracellular analysis of the GABA-induced depolarization in rat dorsal root ganglia. *Brain Research* **118**, 486–493.

DICHTER, M. A. & FISCHBACH, G. D. (1977). The action potential of chick dorsal root ganglion neurones maintained in cell culture. *Journal of Physiology* **267**, 281–298.

DiFrancesco, D. (1981). A new interpretation of the pace-maker current in calf Purkinje fibres. *Journal of Physiology* **314**, 359–376.

Dunlap, K. & Fischbach, G. D. (1981). Neurotransmitters decrease the calcium conductance activated by depolarization of embryonic chick sensory neurones. *Journal of Physiology* **317**, 519–535.

Fenwick, E. M., Marty, A. & Neher, E. (1982). Sodium and calcium channels in bovine chromaffin cells. *Journal of Physiology* **331**, 599–635.

Gallagher, J. P., Higashi, H. & Nishi, S. (1978). Characterization and ionic basis of GABA-induced depolarizations recorded *in vitro* from cat primary afferent neurones. *Journal of Physiology* **275**, 263–282.

Gorke, K. & Pierau, F. K. (1980). Spike potentials and membrane properties of dorsal root ganglion cells in pigeons. *Pflügers Archiv* **386**, 21–28.

Gorman, A. L. F. & Hermann, A. (1979). Internal effects of divalent cations on potassium permeability in molluscan neurones. *Journal of Physiology* **296**, 393–410.

Hamill, O. P., Marty, A., Neher, E., Sakmann, B. & Sigworth, F. J. (1981). Improved patch-clamp techniques for high-resolution current recording from cells and cell-free membrane patches. *Pflügers Archiv* **391**, 85–100.

Ito, M. (1957). The electrical activity of spinal ganglion cells investigated with intracellular microelectrodes. *Japanese Journal of Physiology* **7**, 297–323.

Ito, M. (1959). An analysis of potentials recorded intracellularly from the spinal ganglion cell. *Japanese Journal of Physiology* **9**, 20–32.

Lee, K. S. & Tsien, R. W. (1984). High selectivity of calcium channels in single dialysed heart cells of the guinea-pig. *Journal of Physiology* **354**, 253–272.

MacDonald, J. F. & Schneiderman, J. H. (1984). L-aspartic acid potentiates 'slow' inward current in cultured spinal cord neurones. *Brain Research* **296**, 350–355.

Marty, A., Tan, Y. P. & Trautmann, A. (1984). Three types of calcium-dependent channel in rat lacrimal glands. *Journal of Physiology* **357**, 293–325.

Maruyama, Y. & Petersen, O. H. (1982). Single-channel currents in isolated patches of plasma membrane from basal surface of pancreatic acini. *Nature* **299**, 159–161.

Mayer, M. L. (1985). Calcium-activated chloride current in rat dorsal root ganglion neurones. *Journal of Physiology* **361**, 22*P*.

Mayer, M. L. & Westbrook, G. L. (1983). A voltage-clamp analysis of inward (anomalous) rectification in mouse spinal sensory ganglion neurones. *Journal of Physiology* **340**, 19–45.

Mayer, M. L. & Westbrook, G. L. (1984). Mixed-agonist action of excitatory amino acids on mouse spinal cord neurones under voltage clamp. *Journal of Physiology* **354**, 29–53.

Meech, R. W. (1978). Calcium-dependent potassium activation in nervous tissue. *Annual Review of Biophysics and Bioengineering* **7**, 1–18.

Miledi, R. (1982). A calcium-dependent transient outward current in *Xenopus laevis* oocytes. *Proceedings of the Royal Society* B **215**, 491–497.

Miledi, R. & Parker, I. (1981). Calcium transients recorded with arsenazo III in the presynaptic terminal of the squid giant synapse. *Proceedings of the Royal Society* B **212**, 197–211.

Miledi, R. & Parker, I. (1984). Chloride current induced by injection of calcium into *Xenopus* oocytes. *Journal of Physiology* **357**, 173–183.

Neering, I. R. & McBurney, R. N. (1984). Role for microsomal Ca storage in mammalian neurones? *Nature* **309**, 158–160.

Nowycky, M. C., Fox, A. P. & Tsien, R. W. (1984). Multiple types of calcium channel in dorsal root ganglion cells distinguished by sensitivity to cadmium and single channel properties. *Society for Neurosience Abstracts* **10**, 526.

Owen, D. A., Segal, M. & Barker, J. L. (1984). A Ca-dependent Cl^- conductance in cultured spinal cord neurones. *Nature* **311**, 567–570.

Plant, T. D. & Standen, N. B. (1981). Calcium current inactivation in identified neurones of *Helix aspersa*. *Journal of Physiology* **321**, 273–285.

Ransom, B. R., Neale, E., Henkart, M., Bullock, P. N. & Nelson, P. G. (1977). Mouse spinal cord in cell culture. 1. Morphology and intrinsic neuronal electrophysiological properties. *Journal of Neurophysiology* **40**, 1132–1150.

Smith, S. J., MacDermott, A. B. & Weight, F. F. (1983). Detection of intracellular Ca^{2+} transients in sympathetic neurones using arsenazo III. *Nature* **304**, 350–352.

TEO, T. S. & WANG, J. H. (1973). Mechanism of activation of a cyclic adenosine 3:5-monophosphate phosphodiesterase from bovine heart by calcium ions. *Journal of Biological Chemistry* **248**, 5950–5955.

TILLOTSON, D. & HORN, R. (1978). Inactivation without facilitation of calcium conductance in caesium-loaded neurones of *Aplysia*. *Nature* **273**, 512–514.

YELLEN, G. (1982). Single Ca^{2+}-activated nonselective cation channels in neuroblastoma. *Nature* **296**, 357–359.